Electronic Supplementary Material (ESI) for Journal of Materials Chemistry A.

Electronic Supporting Information

$CuInS_2$/ZnS nanocrystals as sensitisers for NiO photocathodes

Thomas J. Macdonald,[a] Yatin J. Mange, [a] Melissa R. Dewi, [a] Husn U. Islam,[bc] Ivan P. Parkin, [b] William M. Skinner [a] and Thomas Nann [a]*

Mr. Thomas J. Macdonald,[a] Mr. Yatin J. Mange, [a] Dr. Melissa R. Dewi, [a] Ms. Husn U. Islam,[bc] Prof. Ivan P. Parkin, [b] Prof. William M. Skinner [a] and Prof. Thomas Nann* [a]

[a.] T.J. Macdonald, Y.J. Mange, Dr. M.R. Dewi, Prof. W.M. Skinner, Prof. T. Nann
Ian Wark Research Institute, University of South Australia,
Mawson Lakes Blvd, Adelaide, SA 5095,
Australia.
E-Mail: thomas.nann@unisa.edu.au

[b.] Prof. I. P. Parkin, H.U. Islam
Department of Chemistry, University College London,
20 Gordon St, London, WC1H 0AJ
United Kingdom

[c.] H.U. Islam
ESRF
The European Synchrotron
71 Avenue des Martyrs
38000 Grenoble
France

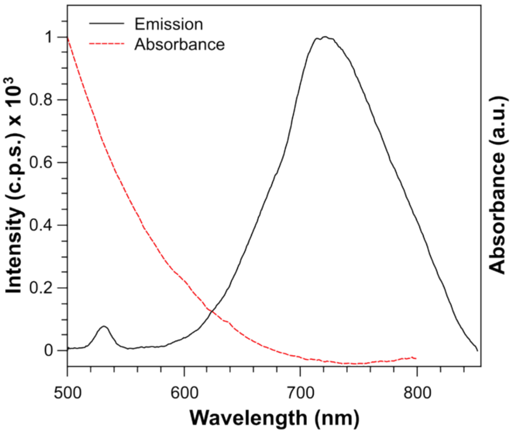

Figure S1. Core $CuInS_2$ Emission and Absorbance Spectra

Figure S1 shows the emission (black) and absorbance (red) for $CuInS_2$ core NCs. The emission spectrum shows a clear defect at approximately 530 nm, which is not present after the NCs are treated with zinc. Furthermore, the absorption of the core NCs is more towards the infrared region as apposed to the zinc treated NCs being more towards the visible region.

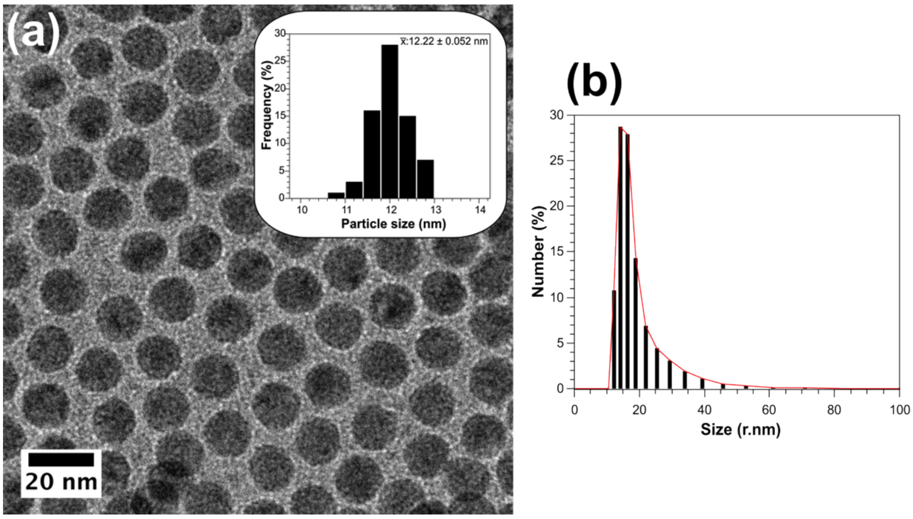

Figure S2. a) TEM of CuInS2/ZnS NCs with 20 nm scale, inset: particle size distribution histogram b) DLS in r.nm for $CuInS_2$/ZnS NCs

Figure S2a shows an additional TEM image over a slightly larger area supporting the size and shape of the NCs. The inset shows a histogram for the average particle size, which was found to be 12.20 ± 0.05 nm. **Figure S2b** shows the DLS for hydrodynamic radius of the NCs, slightly larger sizes may be attributed to the MAA stabilising ligands.

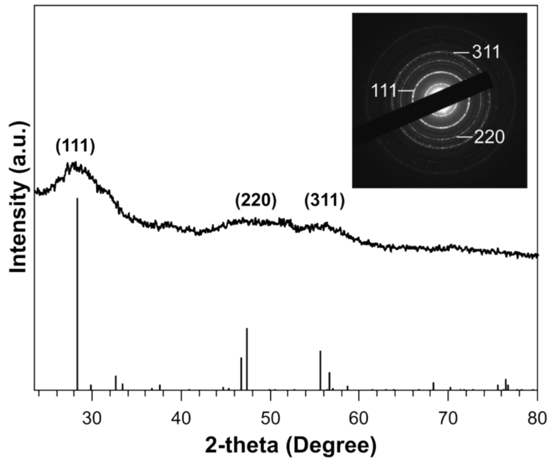

Figure S3. XRD for $CuInS_2$/ZnS NCs and SAED indicating diffraction patterns

The XRD for $CuInS_2$/ZnS NCs with corresponding JCPDS-file 00-047-1372 (roquesite, $CuInS_2$) is shown in **Figure S3**. The SAED with corresponding miller indices for the NCs are shown in the inset.

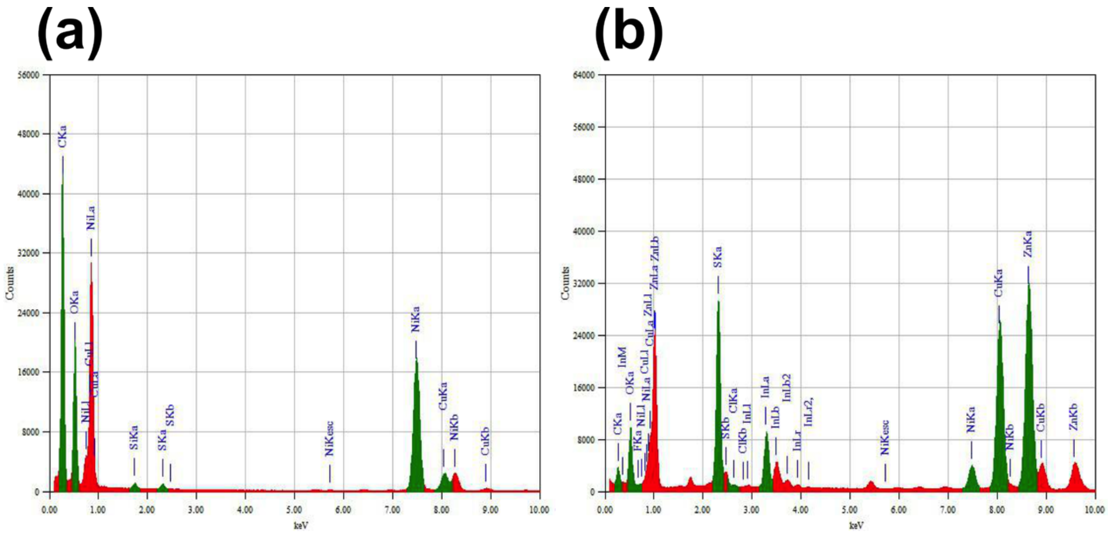

Figure S4. EDXS for bare NiO photocathode films (a) and $CuInS_2$/ZnS NC sensitised films (b)

The EDXS spectroscopy for the unsensitised NiO photocathodes is shown in **Figure S4a**. **Figure S4b** shows the NC sensitised NiO photocathodes revealing the presence of Cu, In, S and Zn. This supports the covalent attachment of the NCs to the NiO photocathodes.

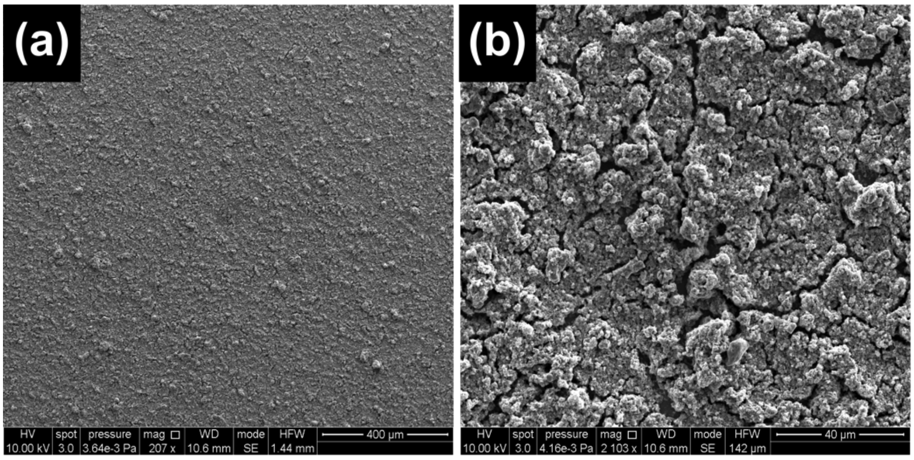

Figure S5. SEM for NiO photocathode films at 400 μM (a) and 40 μM (b)

Figure S5 shows an overview **(a)**, and high resolution **(b)** SEM for the NiO photocathode films. The films show to have some cracking but since the films were several microns thick, the photovoltaic performances of the devices were not affected.

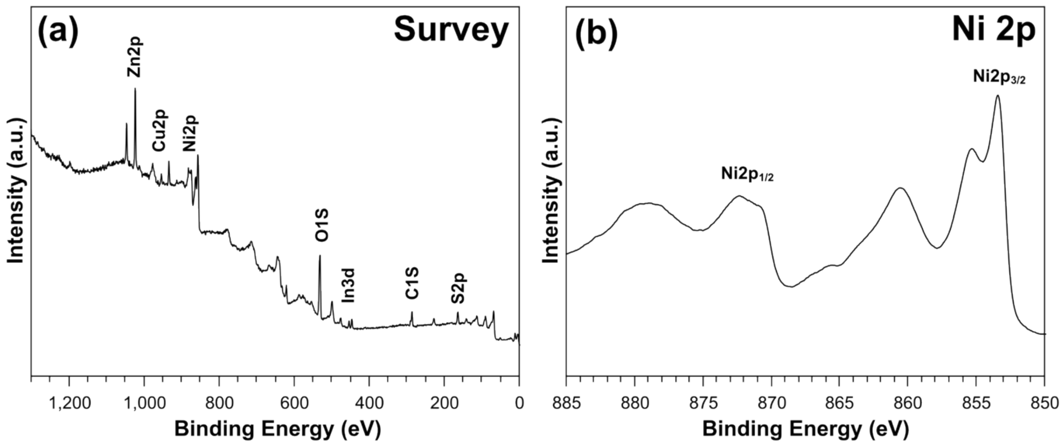

Figure S6. XPS survey spectra for $CuInS_2$/ZnS NCs on NiO Photocathodes, (b) NiO 2p high resolution spectra for bare NiO phocathodes

The XPS survey spectra for the $CuInS_2$/ZnS NC sensitised NiO photocathodes is shown in **Figure S6a**. High resolution Ni 2p XPS for unsensitised NiO photocathodes is shown in **Figure S6b**. The sensitising of NiO photocathodes did not affect he bulk surface properties of the NiO.

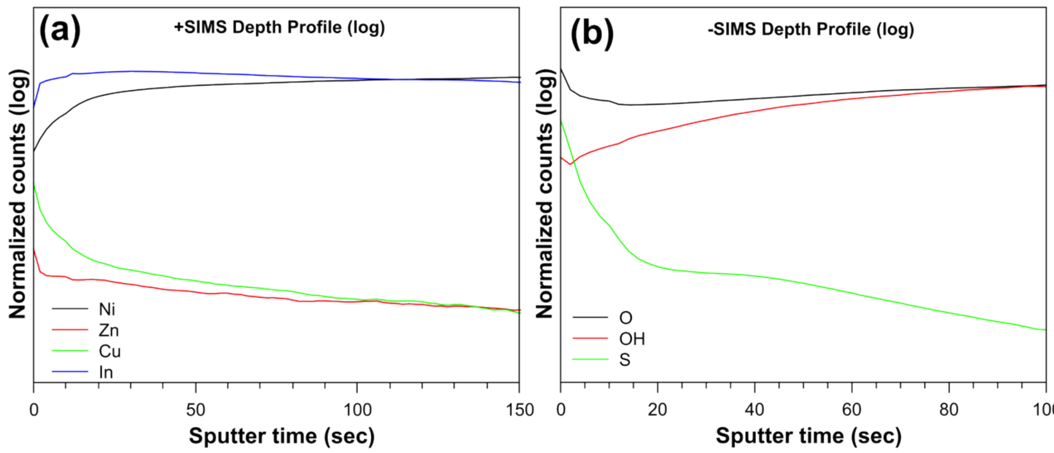

Figure S7. +SIMS depth profile (a) and –SIMS depth profile (b) for $CuInS_2$/ZnS NC sensitised NiO photocathode films.

Figure S7 shows positive **(a)** and negative **(b)** charged depth profiles for the sensitised NiO photocathodes. The ToF-SIMS supports the presence of $CuInS_2$/ZnS NCs to NiO.

S8 a. Redox potentials for photocathode system

The redox potentials for $CuInS_2$/ZnS NCs used in this study were estimated to be E_{CB}($CuInS_2$/ZnS) = -0.5 V and E_{VB}($CuInS_2$/ZnS) = + 1.55 V *vs* NHE. This is with respect to the direct band gap of bulk chalcopyrite ($CuInS_2$) 1.5 eV and CB of 0.3 eV [1,2]. The VB maximum for $CuInS_2$ NCs generally rests 0.2-0.3 eV below that of the selenides making them analogous to systems consisting of the recently studied NiO/CdSe combination [3,4]. The VB of NiO has been reported to be +0.54 V *vs* NHE, which is located between the CB and VB of the synthesised $CuInS_2$/ZnS NCs. In addition, the redox potential of the CB for NiO has been reported to be -3.06 V *vs* NHE, which is above the CB of $CuInS_2$/ZnS NCs [5]. The CB for the NCs is also above that of the iodide/triiodide redox couple (0.35-0.45 eV vs NHE) [6]. An electronic energy diagram is illustrated below, indicating the possible charge transfer processes.

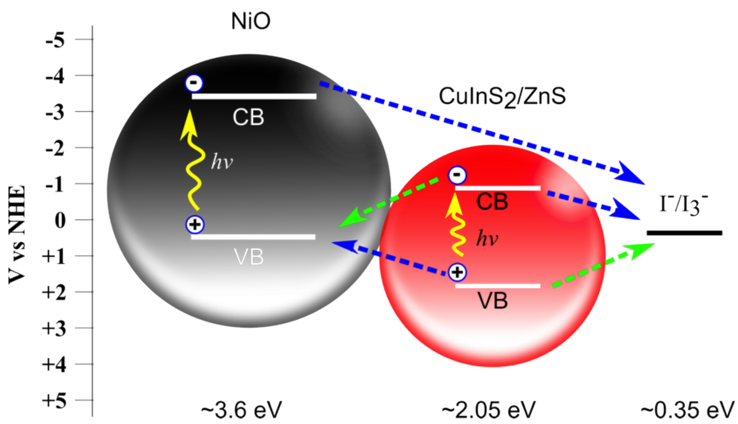

Figure S8 b. Schematic diagram illustrating the charge transfer/recombination processes of the $CuInS_2$/ZnS NC sensitised NiO photocathodes. Upon illumination, a charge transfer takes place from the CB of the CuInS2/ZnS and the NiO (blue lines). The prompts a hole injection from the VB of the NCs to the VB of the NiO. The NCs are subject to recombination that occurs between the NC/redox mediator and the NC/NiO (green lines). Regeneration of NCs occurs by the accepter species I^-.

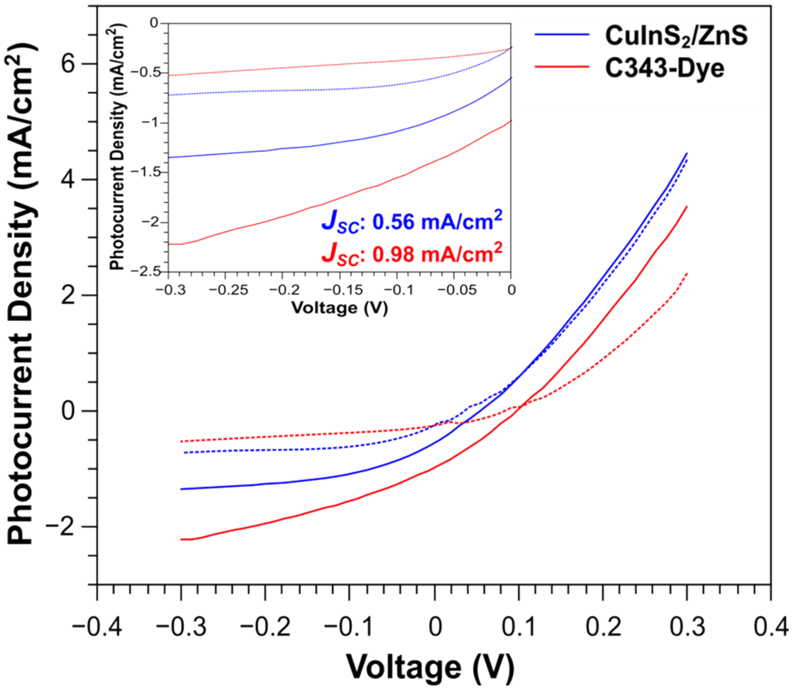

Figure S9. Light *JV*-Curves for $CuInS_2$/ZnS NC sensitised NiO (blue) and C343-Dye sensitised NiO (red). The dark *JV*-Curves are represented by the dotted lines. The J_{SC} values for the NCs and C343-Dye were 0.56 mA/cm^2 and 0.98 mA/cm^2, respectively.

Dark (dotted line) and light (solid line) photocurrents for NC and dye-sensitised NiO photocathodes are shown in **Figure S9**. This confirms the photoresponse from both sensitised photocathodes with respect to their dark currents. Small voltages are present due to the diode characteristics of NiO. The inset shows a zoomed illustration of the dark and light currents from **Figure S9**. High dark currents can be observed and have been previously attributed to the recombination of holes in the NiO with the donor species (I_3^-) in the redox mediator [7].

S10. Stability of NC and C-343 photocathodes

The devices were subject to testing at the end of a working day. The table below shows the average photocurrents for the devices after a 6 hour time period. Generally, the devices maintained good photocurrents throughout the day.

Table S1: 6 Hour stability test for NC and C-343 photocathodes

Sample	V_{OC} (mV)	J_{SC} (mA/cm^2)	*FF* %	*η* %	Rseries (Ohms)
NiO + C343 (6 hour)	0.1	0.95	29	0.03	182
NiO + NCs (6 hour)	0.057	0.52	25	0.01	202

S11. Photovoltaic expressions

$\boldsymbol{J_{SC}}$: Short circuit current density at an applied potential of zero volts
$\boldsymbol{V_{OC}}$: Voltage at open circuit when the cell current is zero

FF: Fill factor is defined as

$$FF = \frac{J_{max}V_{max}}{J_{SC}V_{OC}}$$

$\boldsymbol{\eta}$: Efficiency is defined as

$$\eta = \frac{P_{max}}{P_{in}} = \frac{J_{SC}V_{OC}FF}{P_{in}}$$

References

1. R. Scheer, *Prog. Photovolt. Res. Appl.*, 2012, **20**, 507–511.
2. S. Siebentritt and U. Rau, *Wide-Gap Chalcopyrites*, Springer-Verlag Berlin Heidelberg, 2006, vol. 86.
3. M.-A. Park, S.-Y. Lee, J.-H. Kim, S.-H. Kang, H. Kim, C.-J. Choi and K.-S. Ahn, *Phys. Status Solidi A*, 2014, **211**, 1868–1872.
4. I. Barceló, E. Guillén, T. Lana-Villarreal and R. Gómez, *J. Phys. Chem. C*, 2013, **117**, 22509–22517.
5. J. He, H. Lindström, A. Hagfeldt and S.-E. Lindquist, *J. Phys. Chem. B*, 1999, **103**, 8940–8943.
6. A. Hagfeldt and M. Graetzel, *Chem. Rev.*, 1995, **95**, 49–68.
7. F. Safari-Alamuti, J. R. Jennings, M. A. Hossain, L. Y. L. Yung and Q. Wang, *Phys. Chem. Chem. Phys.*, 2013, **15**, 4767–4774.